Journal of The Electrochemical Society

Electrochemical Activity of Nano-$NiSi_2$ in Li Cells

Electrochemical Activity of Nano-$NiSi_2$ in Li Cells

Zhijia Du,[a] T. D. Hatchard,[b,*] P. Bissonnette,[b] R. A. Dunlap,[a,c,d] and M. N. Obrovac[a,b,c,*,z]

[a]*Department of Physics and Atmospheric Science, Dalhousie University, Halifax, Nova Scotia B3H 4R2, Canada*
[b]*Department of Chemistry, Dalhousie University, Halifax, Nova Scotia B3H 4R2, Canada*
[c]*Institute for Research in Materials, Dalhousie University, Halifax, Nova Scotia B3H 4R2, Canada*
[d]*College of Sustainability, Dalhousie University, Halifax, Nova Scotia B3H 4R2, Canada*

Crystalline and nanocrystalline $NiSi_2$ were studied as negative electrode materials in Li cells. Crystalline $NiSi_2$ was found to be inactive toward lithiation/delithiation. However, it was found that $NiSi_2$ becomes active toward lithium when made nanocrystalline by ball milling. X-ray diffraction peaks from nanocrystalline $NiSi_2$ disappear after the first lithiation process, confirming its electrochemical activity. In subsequent cycles, the voltage curve of nanocrystalline $NiSi_2$ is similar to that of amorphous Si, excepting that there is significant depression of the lithiation potential, which may arise from internal stress.

Manuscript submitted May 31, 2016; revised manuscript received August 10, 2016. Published September 9, 2016.

Si has a high volumetric capacity (2194 mAh/cc,[1] compared to 764 mAh/cc of graphite). Therefore, various Si-based alloys have been investigated in the last two decades to improve the energy density of Li-ion batteries.[1–6] The main idea of using Si-based alloys is to form active/inactive alloys which will dilute the volume expansion of Si during lithiation. The specific design strategy of Si alloys has also been reported.[2] In Si alloys, silicides are usually formed combining Si and other metals. However, conflicting results have been reported in previous studies on the activity of these silicides. The better understanding of their electrochemical performance will contribute to the clarification of transition metal content on capacity.

Kim et al. found that nano-sized crystalline $NiSi_2$ prepared by ball milling $NiSi_2$ had as high as 563 mAh/g reversible capacity and suggested an intercalation mechanism.[7] Wang et al. and Zhou et al. reported that NiSi prepared by ball milling and laser deposition had capacities of 1180 mAh/g and 1220 mAh/g, respectively.[8,9] Both these results were explained by the fact that NiSi reacts reversibly with Li to form lithiated silicon and Ni. In contrast to these studies, researchers have reported silicides may have little to no activity versus Li. Huggins et al found capacities of 58, 60, and 198 mA h/g for $CoSi_2$, $FeSi_2$, and $NiSi_2$, respectively.[10] Dong et al.[11] declared $FeSi_2$ to be inactive, since $FeSi_2$ XRD peaks did not shift during the lithiation/delithiation process. Similarly, Park et al. reported that the $NiSi_2$ phase was also inactive because its XRD peaks were unchanged during cycling between 5 mV and 1.5 V.[12]

Recently, we have studied the electrochemical behavior of ball milled Ni_xSi_{1-x} alloys.[13] These alloys were found to consist of nanocrystalline Si and $NiSi_2$ for $0 < x \leq 0.30$. However, the reversible capacity dependence on x is not consistent with the hypothesis that $NiSi_2$ is inactive. Instead, the capacity was consistent with the formation of nanocrystalline Si as an active phase and NiSi as an inactive phase during cycling. This indicates that the $NiSi_2$ phase in ball milled Ni-Si alloys has appreciable capacity. In these alloys capacity was further reduced by the depression of the voltage curve, which we suggested was due to stress-voltage coupling.[13]

The different preparation methods in the above studies result in different microstructures and are likely the cause of the disparate reaction mechanisms. In the present study, crystalline $NiSi_2$ (c-$NiSi_2$) and nanocrystalline $NiSi_2$ (n-$NiSi_2$) are prepared and their behavior as anodes in Li-ion cells is studied to better understand the effect of microstructure on their electrochemistry. In addition, X-ray diffraction is used to study the mechanisms of lithiation.

Experimental

c-$NiSi_2$ was prepared by arc-melting stoichiometric amounts of Ni (sphere, 99.95+%, Aldrich Chemical Co.) and Si (lump, 98.4%, Alfa Aesar) in an Ar atmosphere, grinding the resulting ingot by hand with a mortar and pestle, and then annealing at 950°C for 10 hours under Argon flow with titanium sponge getters placed upstream in the hot zone to remove any oxygen impurity. Ball milled $NiSi_2$ was prepared by sealing 2 grams of the obtained c-$NiSi_2$ alloy powders with 40 grams of 0.25 inch stainless steel balls under Argon atmosphere in a 40 ml hardened steel vial and ball milling 4 hours in a SPEX 8000 M Mixer/Mill. Some ball milled samples were subsequently heated at temperatures from 300 - 600°C for 12 hours under argon flow. X-ray diffraction patterns were collected using a JD2000 diffractometer equipped with a Cu Kα X-ray source and a diffracted beam monochromator. Sample morphology was studied using a Phenom G2 pro desktop scanning electron microscope (SEM).

Electrode slurries were made by mixing $NiSi_2$ samples, carbon black (from Super P, Erachem Europe) and a 10 weight % aqueous solution of lithium polyacrylate (LiPAA) with a volumetric ratio of 80/5/15 in distilled water. The mixing was conducted in a PM200 Planetary Ball Mill with 4 WC balls (the ball/sample weight ratio was 15:1) at 100 rpm for a period of 1 h. The slurries were coated on electrolytic Cu foil (Furukawa Electric, Japan) using a 0.004 inch gap coating bar and dried at 120°C in air for 1 h.

Electrodes were assembled in 2325-type coin cells with a lithium foil counter/reference electrode. Two layers of Celgard 2300 separator were used in each coin cell. 1 M $LiPF_6$ (BASF) in a solution of ethylene carbonate, diethyl carbonate and monofluoroethylene carbonate (volume ratio 3:6:1, all from BASF) was used as electrolyte. Cells were cycled galvanostatically at 30.0 ± 0.1°C between 5 mV and 0.9 V using a Maccor Series 4000 Automated Test System at a C/20 rate for the first cycle and a C/10 rate for the following cycles with a C/40 trickle discharge (lithiation).

Results

Figures 1a and 1b show the morphologies of c-$NiSi_2$ made from high temperature processing and n-$NiSi_2$ made by ball milling the c-$NiSi_2$ powder, respectively. Bulk chunks with sharp edges and sizes ranging from 10–20 μm are the dominant features with a small quantity of smaller pieces. After ball milling, the particle size is significantly reduced to the range of 1–5 μm. Figure 2 shows the XRD patterns of c-$NiSi_2$ and n-$NiSi_2$. The c-$NiSi_2$ sample has very sharp and well defined diffraction peaks, while the n-$NiSi_2$ sample has broad peaks, indicating that ball milling has changed the sample microstructure from crystalline to a nanocrystalline/amorphous state. The

*Electrochemical Society Member.
[z]E-mail: mnobrovac@dal.ca

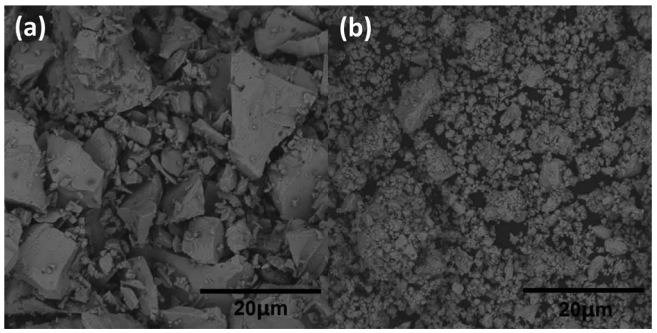

Figure 1. SEM images of (a) c-$NiSi_2$ and (b) n-$NiSi_2$ powders.

crystallite sizes of c-$NiSi_2$ and n-$NiSi_2$ were determined to be 66.1 nm and 4.2 nm, respectively, based on the Scherrer equation applied to the (200) peak at 47.6°.

Figure 3 shows the voltage curves of c-$NiSi_2$ and n-$NiSi_2$ electrodes. The c-$NiSi_2$ electrode is essentially inactive toward lithium. In contrast, the n-$NiSi_2$ electrode shows appreciable capacity during lithiation/delithiation. The first lithiation voltage is very low compared to the following cycles, indicating slow initial lithiation kinetics. The charge capacity gradually increases from 313 mAh/g to 345 mAh/g during cycles 1–5. This "activation" process for the early cycles is likely due to the gradual breakdown of the alloy microstructure during lithiation/delithiation, resulting in improved access of portions of the alloy particle toward lithiation as cycling proceeds. However, the exact reason needs further investigation. Figure 4 shows the differential capacity curves of the n-$NiSi_2$ electrode in Figure 3 for the first three cycles. No appreciable change in differential capacity features were observed during subsequent cycling. The differential capacity curves are very similar to the ball milled $Ni_{0.35}Si_{0.65}$ samples in our previous study.[13] In our recent papers on sputtered and ball milled Ni-Si alloys,[13,14] we have found that inactive alloy components depress the lithiation voltage of Si. We suggested that this was because these inactive components applied stress to the active Si phase as it expands during lithiation. For the n-$NiSi_2$ electrode, two broad peaks during lithiation/delithiation (marked as A/A' and B/B') are characteristic of amorphous Si. As suggested in References 13 and 14, internal stress in the alloy from the presence of Ni results in the lithiation voltage being shifted toward lower potentials. This results in the truncation of peak B at 5 mV and limits the alloy capacity.

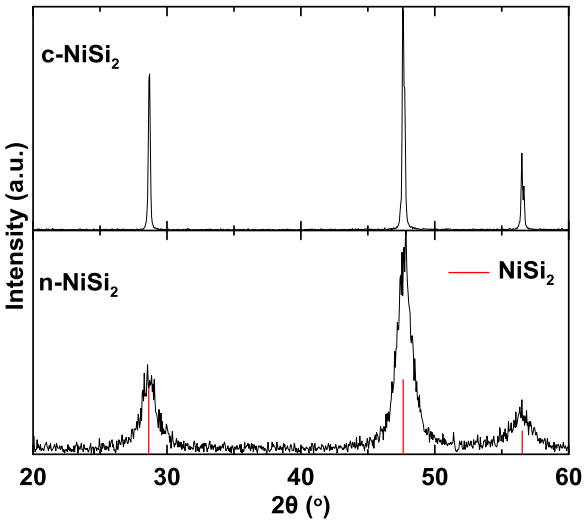

Figure 2. XRD patterns of c-$NiSi_2$ and n-$NiSi_2$.

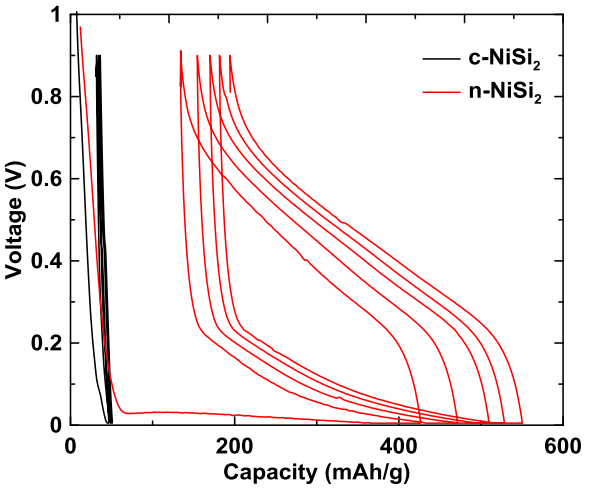

Figure 3. Voltage curves of c-$NiSi_2$ and n-$NiSi_2$ electrodes.

Figure 5 shows an ex-situ XRD pattern of the n-$NiSi_2$ electrode after being fully lithiated to 5 mV. The lithiated sample is completely amorphous with almost no $NiSi_2$ peaks. This confirms that n-$NiSi_2$ is active and implies that the nanoscale crystal size of $NiSi_2$ facilitates its reaction with lithium and leads to appreciable capacity. The result indicates that other transition metal silicides should be carefully studied for their lithiation/delithiation reactivity when they are in nanocrystalline state. To further confirm the reaction between n-$NiSi_2$ and lithium, in-situ XRD measurements were performed for the $Ni_{0.25}Si_{0.75}$ alloy electrode from [Ref 9] at different discharge/charge states. The resulting XRD patterns are shown in Figure 6. Broad peaks from $NiSi_2$ can be seen in the XRD patterns of the cell prior to cycling at open circuit. The broad peak at about 28° is somewhat obscured by a sharper peak from a cell part that is at the same angle. During the first discharge, the intensity of the $NiSi_2$ peaks gradually decrease with voltage, indicating that $NiSi_2$ and Li react to make an amorphous product. During charge the $NiSi_2$ peaks do not reappear. Either $NiSi_2$ is not reformed during delithiation or it is amorphous.

The effect of the $NiSi_2$ grain size on its ability to react with lithium was investigated by annealing ball milled n-$NiSi_2$ to different temperatures. XRD patterns of annealed n-$NiSi_2$ samples are shown in Figure 7. As the annealing temperature is increased, the XRD peaks narrow, indicating grain growth. These XRD patterns were fit by Rietveld refinement. Since ball milling can produce metastable samples, the fits included the possibility of a Si impurity phase being present. The results of the refinements are listed in Table I. The Bragg R (R_B)

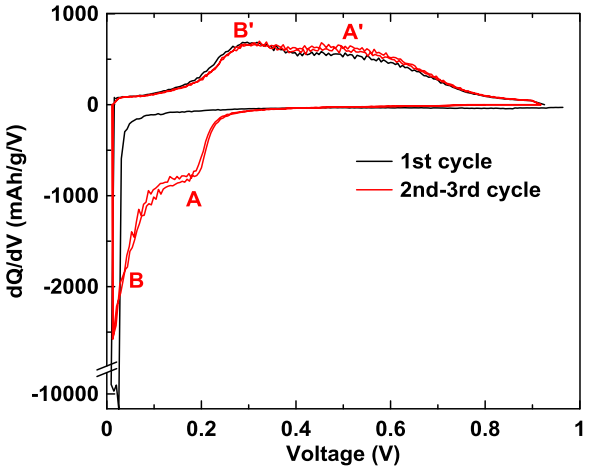

Figure 4. Differential capacity curves of n-$NiSi_2$ for the first 3 cycles.

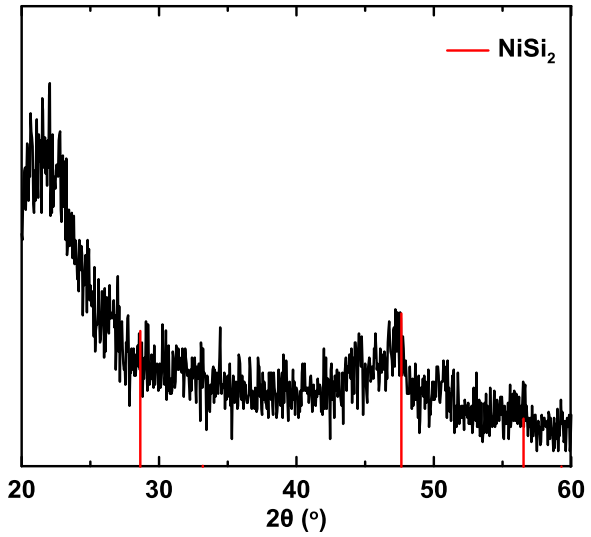

Figure 5. XRD pattern of a n-$NiSi_2$ electrode after the first lithiation to 5 mV.

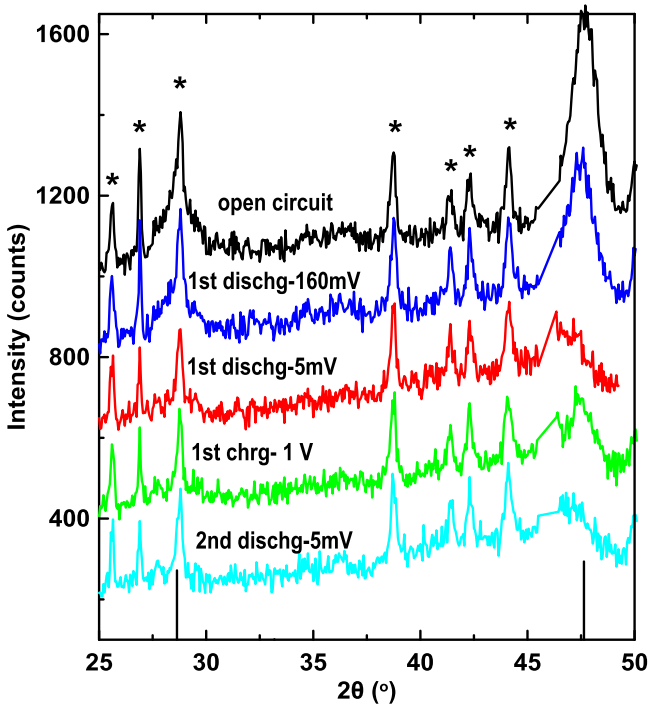

Figure 6. In-situ XRD patterns of $Ni_{0.25}Si_{0.75}$ electrodes during lithiation and delithiation, the discharge/charge state is indicated in the figure. The patterns are off-set by 200 counts for clarity. Diffraction peaks from $NiSi_2$ are indicated with black vertical lines at 28.6° and 47.6°. All other sharp peaks, marked with asterisks, originate from cell parts.

Table I. Results of Rietveld refinements of $NiSi_2$ samples made by ball milling cr-$NiSi_2$ and then annealing at different indicated temperatures. (R_B = Bragg R, GOF = goodness of fit).

Sample	Mol % $NiSi_2$	Mol % Si	R_B ($NiSi_2$)	R_B (Si)	GOF
RT	89	11	3.47	3.03	1.509
300°C	92	8	1.61	5.88	2.573
400°C	100	0	3.04	N/A	1.777
500°C	100	0	1.87	N/A	1.707
600°C	98	2	1.82	15.12	1.743

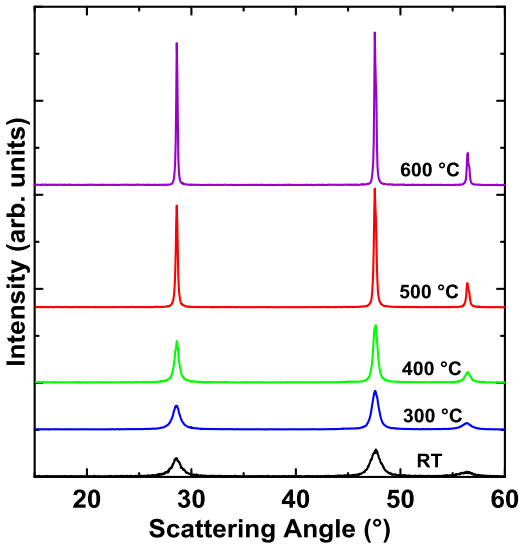

Figure 7. XRD patterns of n-$NiSi_2$ samples after annealing at different temperatures.

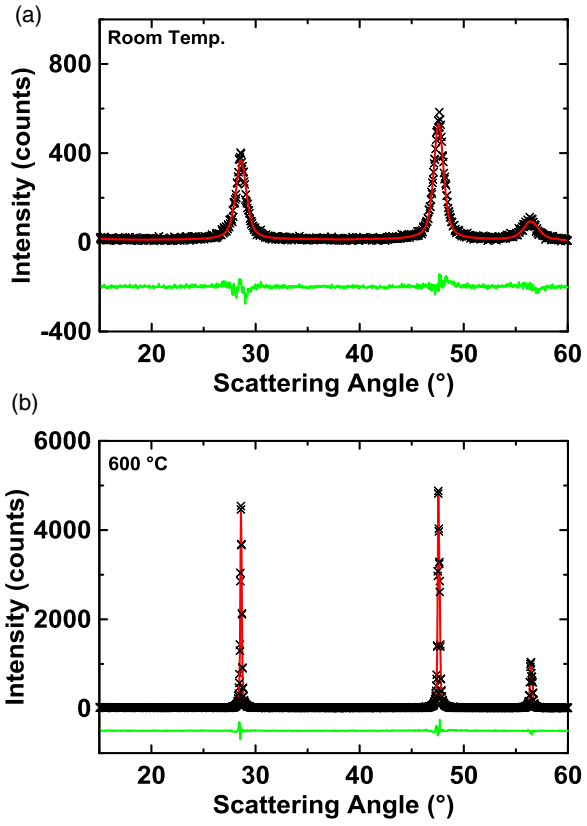

Figure 8. Rietveld refinements of (a) n-$NiSi_2$ and (b) n-$NiSi_2$ after annealing to 600°C. Differences between the refined pattern and the observed pattern are shown at the bottom of each panel.

of the majority $NiSi_2$ phase is about 2 - 3.5 for all samples, indicating a good fit. A good fit for the Si phase (R_B < 5) was only obtained for the as milled samples, which contained a significant quantity of this phase (11% by Rietveld refinement). For the other samples, the amount of this phase was much less and therefore the error in fitting this phase increased. Nevertheless an excellent overall goodness of fit was obtained for all samples. Figure 8 shows the Rietveld refinements of the unheated sample and the sample heated to 600°C. Improved

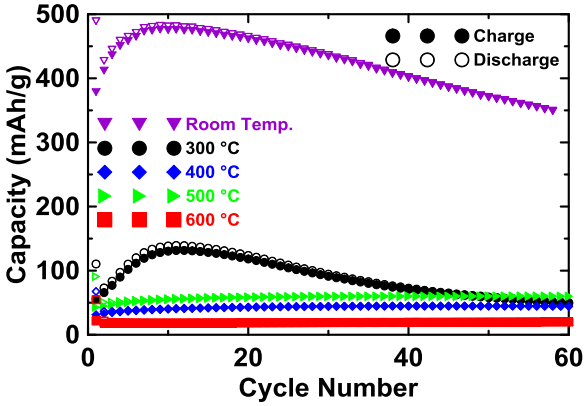

Figure 9. Cycling performance of n-$NiSi_2$ and annealed n-$NiSi_2$ samples.

fits were only obtained if the Si impurity was included for the n-$NiSi_2$ sample and the sample heated to 300°C. However, the amount of the Si impurity was small. At higher temperatures, the refinements resulted in the amount of Si impurity to be zero or near zero. This is consistent with these samples reaching thermal equilibrium, as predicted by the Ni-Si binary phase system. As the annealing temperature is increased the grain size increases from 6.6 nm to 66.7 nm.

Figure 9 shows the cycling performance of the n-$NiSi_2$ sample and annealed n-$NiSi_2$ samples. The n-$NiSi_2$ sample has an initial capacity of about 400 mAh/g, which increases to 489 mAh/g after 10 cycles. As mentioned above, electrochemical activation may improve access to more parts of the alloy during cycling, resulting in an increased capacity. After cycle 10, the n-$NiSi_2$ capacity begins to fade. The capacity of the 300°C annealed n-$NiSi_2$ is greatly reduced from the annealed sample, but follows the same general trend. The mechanism of the fade process is not clear, since alloys with much greater volume expansion have been shown to have almost no fade in the same number of cycles. Indeed, the volume expansion of the 300°C annealed sample is only about 30%, by the analysis described in Reference 2. At higher annealing temperatures the alloy capacity becomes small and most of the capacity observed is from the carbon black in the coating.

These results are summarized in Figure 10, which shows the dependence of the maximum delithiation capacity observed during cycling and the grain size with annealing temperature. The grain size only increases slightly below 400°C. Nevertheless, the capacity dramatically

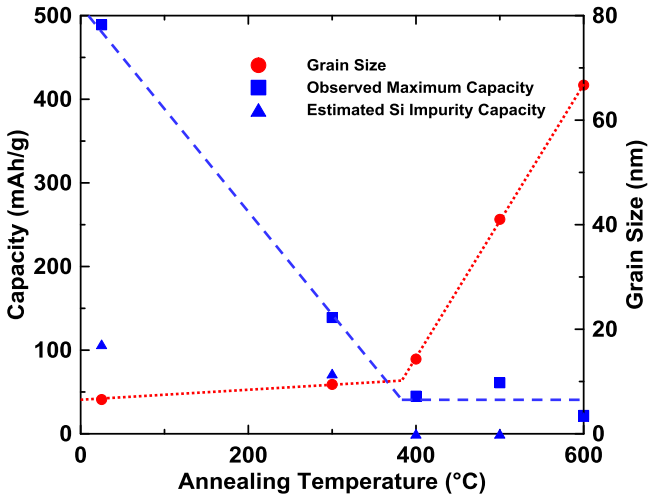

Figure 10. The dependence of the capacity and grain size of n-$NiSi_2$ on annealing temperature. Dashed lines are added as a guide to the eye. The estimated capacity from a possible Si impurity as predicted by Rietveld refinement is also shown.

decreases. This suggests that the electrochemical activity of $NiSi_2$ is highly sensitive to sample crystallinity/grain size. At annealing temperatures of 400°C and above, the grain size increases significantly and the lithiation capacity of $NiSi_2$ becomes negligible. Also shown in Figure 10 are the capacity contributions from a Si impurity phase based on Rietveld refinement results. The amount of capacity that might come from a Si impurity phase is much less than is observed, further supporting the XRD findings that the $NiSi_2$ phase must be active to explain the observed capacity.

Discussion

The XRD results that show the disappearance of the $NiSi_2$ phase during lithiation and the much greater observed capacity compared to what could be expected from any Si impurities strongly support the conclusion that the n-$NiSi_2$ phase is electrochemically active. Since the differential capacity after the first cycle is identical to that of pure Si, this suggests that a displacement reaction occurs during the first lithiation of n-$NiSi_2$:

$$2xLi + n\text{-}NiSi_2 \rightarrow Ni + 2Li_xSi \quad [1]$$

The theoretical capacity for the above reaction is 1750 mAh/g, assuming the formation of $Li_{15}Si_4$ at full lithiation. However, a much reduced capacity is observed. This suggests that this reaction must be kinetically limited, and explains why lithiation occurs for n-$NiSi_2$ and is greatly impeded or stopped when n-$NiSi_2$ samples are annealed to increase grain size.

The poor cycling performance of n-$NiSi_2$ shown in Figure 9 is more difficult to explain, considering that the volume expansion in these alloys is relatively low. The initially increasing capacity suggests that more $NiSi_2$ material is being accessed during every cycle. It can also be seen from Figure 9 that for each cycle the lithiation capacity is significantly higher than the subsequent delithiation capacity, especially for the first 20 cycles. This suggests that at the same time some active material is lost, likely from mechanical disconnection. These two effects when combined would give rise to the shape of the capacity versus cycle number plot, which rises a maximum value followed by capacity fade. It may be that the extrusion of the product phases, a process that necessarily accompanies displacement reactions, causes mechanical failure, resulting in capacity fade. If that is the case, then materials that undergo such reactions should be avoided in the design of long cycle life alloy negative electrode materials.

Thermodynamically, c-$NiSi_2$ should react with lithium. Therefore, its inability to react must be kinetic in nature. Based on this, we have considered two possible explanations that might account for the strong dependence of the electrochemical activity of $NiSi_2$ with grain size. Firstly, the introduction of grain boundaries with decreasing grain size may increase Li diffusion and thus enable lithiation. Another possible explanation may be related to surface energy. As the grains become smaller, the surface energy of each grain would increase compared to the bulk. This can result in increased bond lengths and a decreased melting point of nanoparticles. These effects may lower activation barriers and enable lithium insertion. Whatever the reason, it is important to note that many Si-transition metal alloys are predicted to react with lithium by thermodynamics, but do not. Therefore, it is important to investigate if other intermetallic compounds of Si can become active when their grain size is reduced.

Conclusions

Crystalline and nanocrystalline phase $NiSi_2$ were prepared by annealing and ball milling. Their activity with Li was evaluated in Li half-cells. No capacity was observed for crystalline $NiSi_2$ electrodes while nanocrystalline $NiSi_2$ electrodes has a maximum reversible capacity of almost 500 mAh/g. XRD studies confirmed that nanocrystalline $NiSi_2$ reacted with lithium and changed into completely amorphous state. The first lithiation voltage is very low compared to following cycles. After the first cycle, the lithiation/delithiation process showed typical feature of amorphous Si alloys. Truncation of dQ/dV curve

due to voltage suppression was also observed in nanocrystalline $NiSi_2$ electrode, confirming previous studies.[13,14] The result suggested that other transition metal silicides should be further studied for their lithium activity.

Acknowledgments

The authors acknowledge funding from NSERC and 3 M Canada, Co. under the auspices of the Industrial Research Chair and Discovery grant programs. We also acknowledge the support of the Canada Foundation for Innovation, the Atlantic Innovation Fund and other partners that fund the Facilities for Materials Characterization managed by the Institute for Research in Materials. ZD acknowledges financial support from the Killam Trusts.

References

1. M. N. Obrovac and L. Christensen, *Electrochem. Solid-State Lett.*, **7**, A93 (2004).
2. M. N. Obrovac, L. Christensen, Dinh Ba Le, and J. R. Dahn, *J. Electrochem. Soc.*, **154**, A849 (2007).
3. Dominique Larcher, Shane Beattie, Mathieu Morcrette, Kristina Edström, Jean-Claude Jumas, and Jean-Marie Tarascon, *J. Mat. Chem.*, **17**, 3759 (2007).
4. Cheol-Min Park, Jae-Hun Kim, Hansu Kim, and Hun-Joon Sohn, *Chem. Soc. Rev.*, **39**, 3115 (2010).
5. Matthew T. McDowell, Seok Woo Lee, William D. Nix, and Yi Cui, *Adv. Mater.*, **25**, 4966 (2013).
6. Uday Kasavajjula, Chunsheng Wang, and A. John Appleby, *J. Power Sources*, **163**, 1003 (2007).
7. M. J. Kim, D. G. Kim, and H.-J. Sohn, *NiSi2 Alloy as an Anode Materials for Lithium-ion Batteries*, *202nd Meeting of the Electrochemical Society*, 2002, Abstract #18.
8. G. X. Wang, L. Sun, D. H. Bradhurst, S. Zhong, S. X. Dou, and H. K. Liu, *J. Power Sources*, **88**, 278 (2000).
9. Y.-N. Zhou, W.-J. Li, H.-J. Chen, C. Liu, L. Zhang, and Z. Fu, *Electrochem. Comm.*, **13**(6), 546 (2011).
10. A. Netz, R. A. Huggins, and W. Weppner, *J. Power Sources*, **119-121**, 95 (2003).
11. H. Dong, X. P. Ai, and H. X. Yang, *Electrochem. Commun.*, **5**, 952 (2003).
12. M.-S. Park, Y.-J. Lee, S. Rajendran, M.-S. Song, H.-S. Kim, and J.-Y. Lee, *Electrochim. Acta*, **50**(28), 5561 (2005).
13. Zhijia Du, Sarah Ellis, R. A. Dunlap, and M. N. Obrovac, *J. Electrochem. Soc.*, **163**(2), A13 (2016).
14. Z. Du, T. D. Hatchard, R. A. Dunlap, and M. N. Obrovac, *J. Electrochem. Soc.*, **162**(9), A1858 (2015).